INTERNATIONAL JOURNAL FOR NUMERICAL METHODS IN FLUIDS, VOL. 8, 559–578 (1988)

BOUNDARY-TYPE FINITE ELEMENT METHOD FOR WAVE PROPAGATION ANALYSIS

MUTSUTO KAWAHARA, HIDEYUKI SAKURAI AND KAZUO KASHIYAMA

Department of Civil Engineering, Chuo University, Kasuga, Bunkyo-ku, Tokyo, Japan

SUMMARY

The boundary-type finite element method has been investigated and applied to the Helmholz and mild-slope equations. Four types of interpolation function are examined based on trigonometric function series. Three-node triangular, four-node quadrilateral, six-node triangular and eight-node quadrilateral elements are tested; these are all non-conforming elements. Three types of numerical example show that the three-node triangular and four-node quadrilateral elements are useful for practical analysis.

KEY WORDS Boundary-type finite element method Helmholz equation Mild-slope equation

INTRODUCTION

The purpose of this paper is to investigate solution procedures for wave propagation by the boundary-type finite element method, which was originally presented by our research group and applied to the Helmholz and mild-slope equations. The validity of the method is shown in the numerical examples given in References 1–5.

The procedure is based on the following ideas. The variational form of the basic equation can be formulated as the boundary integral equation assuming that the interpolation equation satisfies the basic equation. For this purpose, this paper employs four types of sinusoidal function series. The final finite element equation can be obtained by performing a line integral for each finite element and superposing the resulting equations with the total nodal points in the wave field to be analysed.

The characteristic features of this method are as follows:

(i) The method succeeds in avoiding the singularity property although it employs almost the same procedure as the boundary element method. The singularity property must be avoided in the numerical analysis if it can because the numerical analysis is performed using finite decimals and the number of computation digits is limited.

(ii) A coarser finite element mesh can be used more effectively than the ordinary mesh employed in the conventional finite element method. It is necessary to divide the field into a number of finite elements to solve the problem because the present method employs an approximate solution. The number of elements can be reduced.

(iii) Computation time can be saved because the integration is carried out using only line integrals.

In previous papers we have presented the method based on the three-node triangular and four-node quadrilateral elements. In this paper the interpolation equations based on the six-node

0271–2091/88/050559–20$10.00

Received June 1985
Revised 5 June 1987

triangular and eight-node quadrilateral elements are examined. The interpolation equations used in the present paper are all non-conforming. Wave propagation phenomena over the surface of constant-depth and inclined-bottom channels and the oscillation of Ohfunato Bay are computed as numerical investigations. The results show that the three-node triangular and four-node quadrilateral elements are superior to the higher-order elements. The oscillation resonance curve computed via the three- and four-node elements is in good agreement with the observed curve. The present method has been shown to be useful for practical applications.

BOUNDARY-TYPE FINITE ELEMENT METHOD

The boundary-type finite element method has been presented and examined previously by our research group. The precise formulations can be found in References 1–5. The mild-slope equation is used as the basic equation:[6,7]

$$(CC_g\eta_{,i})_{,i}+\omega^2(C_g/C)\eta=0 \qquad \text{in V}, \tag{1}$$

when η is the water elevation and C and C_g represent the phase velocity and group velocity respectively. The angular frequency ω is derived from the dispersion relation

$$\omega^2=gk\tanh(kh) \tag{2}$$

where k, g and h are the wave number, gravitational acceleration and the water depth respectively. On the boundary S of the domain V the following two boundary conditions are introduced:

$$\eta=\hat{\eta} \qquad \text{on } S_1, \tag{3}$$

$$\eta_{,n}=\partial\eta/\partial n=\hat{\eta}_{,n} \quad \text{on } S_2, \tag{4}$$

where n is the unit normal to the boundary and superscript $\hat{}$ denotes the value which is specified on the boundary S. The whole boundary consists of S_1 and S_2 only and there is no overlap between S_1 and S_2.

Assuming that the interpolation equation for the water elevation satisfies the Helmholz equation in each finite element, the function Π to be minimized is written in the form

$$\Pi=\tfrac{1}{2}\int_s(CC_g\eta\eta_{,n})\mathrm{d}s-\int_{s_2}(CC_g\eta\hat{\eta}_{,n})\mathrm{d}s. \tag{5}$$

The wave field to be analysed is divided into a large number of finite elements, the interpolation of which can be written as

$$\eta=\mathbf{P}\{\alpha\}, \tag{6}$$

where $\mathbf{P}$ denotes the interpolation equation, which is discussed precisely in the next section, and $\{\alpha\}$ represents the undetermined constants. The fact that the wave elevation should coincide with the wave elevation at each nodal point leads to

$$\{\tilde{\eta}\}=\mathbf{G}\{\alpha\}, \tag{7}$$

where $\{\tilde{\eta}\}$ denotes the water elevation at each nodal point of the finite elements. Using equations (6) and (7), the following is obtained:

$$\eta=\mathbf{P}\mathbf{G}^{-1}\{\tilde{\eta}\}, \tag{8}$$

$$\eta_{,n}=\frac{\partial}{\partial n}\mathbf{P}\{\alpha\}=\mathbf{Q}\mathbf{G}^{-1}\{\tilde{\eta}\}. \tag{9}$$

Introducing equations (8) and (9) into equation (5) and using the stationary condition of the function Π, the equation for the boundary-type finite element method can be derived as

$$\mathbf{K}\{\eta\}=\{F\} \tag{10}$$

where

$$\mathbf{K}=(\mathbf{G}^{-1})^{\mathrm{T}}\mathbf{D}\mathbf{G}^{-1},$$

$$\mathbf{D}=\tfrac{1}{2}\int_s CC_g(\mathbf{P}^{\mathrm{T}}\mathbf{Q}+\mathbf{Q}^{\mathrm{T}}\mathbf{P})\mathrm{d}s,$$

$$\{F\}=\mathbf{G}^{-1}\int_{s_2} CC_g\mathbf{P}^{\mathrm{T}}\hat{\eta}_{,n}\mathrm{d}s.$$

The usual superposition procedures based on equation (10) lead to the global form of the boundary-type finite element method.

INTERPOLATION EQUATION

Four types of element and five equations are introduced as the interpolation equation for the comparative study. These are based on trigonometric function series and are written as follows. The first equation is the function $\mathbf{P}$ in equation (6) expressed as

$$\mathbf{P}=\left[\cos\left(\frac{k}{\sqrt{2}}x\right)\cos\left(\frac{k}{\sqrt{2}}y\right)\quad\cos\left(\frac{k}{\sqrt{2}}x\right)\sin\left(\frac{k}{\sqrt{2}}y\right)\quad\sin\left(\frac{k}{\sqrt{2}}x\right)\cos\left(\frac{k}{\sqrt{2}}y\right)\right], \tag{11}$$

based on the three-node triangular element. The second equation is

$$\mathbf{P}=\left[\cos\left(\frac{k}{\sqrt{2}}x\right)\cos\left(\frac{k}{\sqrt{2}}y\right)\quad\cos\left(\frac{k}{\sqrt{2}}x\right)\sin\left(\frac{k}{\sqrt{2}}y\right)\right.$$
$$\left.\sin\left(\frac{k}{\sqrt{2}}x\right)\cos\left(\frac{k}{\sqrt{2}}y\right)\quad\sin\left(\frac{k}{\sqrt{2}}x\right)\sin\left(\frac{k}{\sqrt{2}}y\right)\right], \tag{12}$$

based on the four-node quadrilateral element. The third and fourth equations are

$$\mathbf{P}=\left[\cos\left(\frac{k}{\sqrt{2}}x\right)\cos\left(\frac{k}{\sqrt{2}}y\right)\quad\cos\left(\frac{k}{\sqrt{2}}x\right)\sin\left(\frac{k}{\sqrt{2}}y\right)\right.$$
$$\left.\sin\left(\frac{k}{\sqrt{2}}x\right)\cos\left(\frac{k}{\sqrt{2}}y\right)\quad\sin\left(\frac{k}{\sqrt{2}}x\right)\sin\left(\frac{k}{\sqrt{2}}y\right)\quad\cos(kx)\quad\cos(ky)\right] \tag{13}$$

and

$$\mathbf{P}=\left[\cos\left(\frac{k}{\sqrt{2}}x\right)\cos\left(\frac{k}{\sqrt{2}}y\right)\quad\sin\left(\frac{k}{\sqrt{2}}x\right)\sin\left(\frac{k}{\sqrt{2}}y\right)\quad\cos(kx)\quad\cos(ky)\quad\sin(kx)\quad\sin(ky)\right], \tag{14}$$

based on the six-node triangular finite element. The fifth equation is

$$\mathbf{P}=\left[\cos\left(\frac{k}{\sqrt{2}}x\right)\cos\left(\frac{k}{\sqrt{2}}y\right)\quad\cos\left(\frac{k}{\sqrt{2}}x\right)\sin\left(\frac{k}{\sqrt{2}}y\right)\right.$$
$$\left.\sin\left(\frac{k}{\sqrt{2}}x\right)\cos\left(\frac{k}{\sqrt{2}}y\right)\quad\sin\left(\frac{k}{\sqrt{2}}x\right)\sin\left(\frac{k}{\sqrt{2}}y\right)\quad\cos(kx)\quad\cos(\mathrm{k}y)\quad\sin(kx)\quad\sin(ky)\right], \tag{15}$$

based on the eight-node quadrilateral element. There is a wide variety of possibilities for selecting

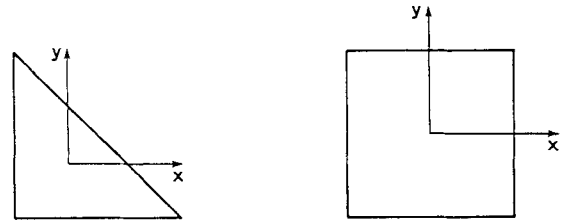

Figure 1. Co-ordinate system

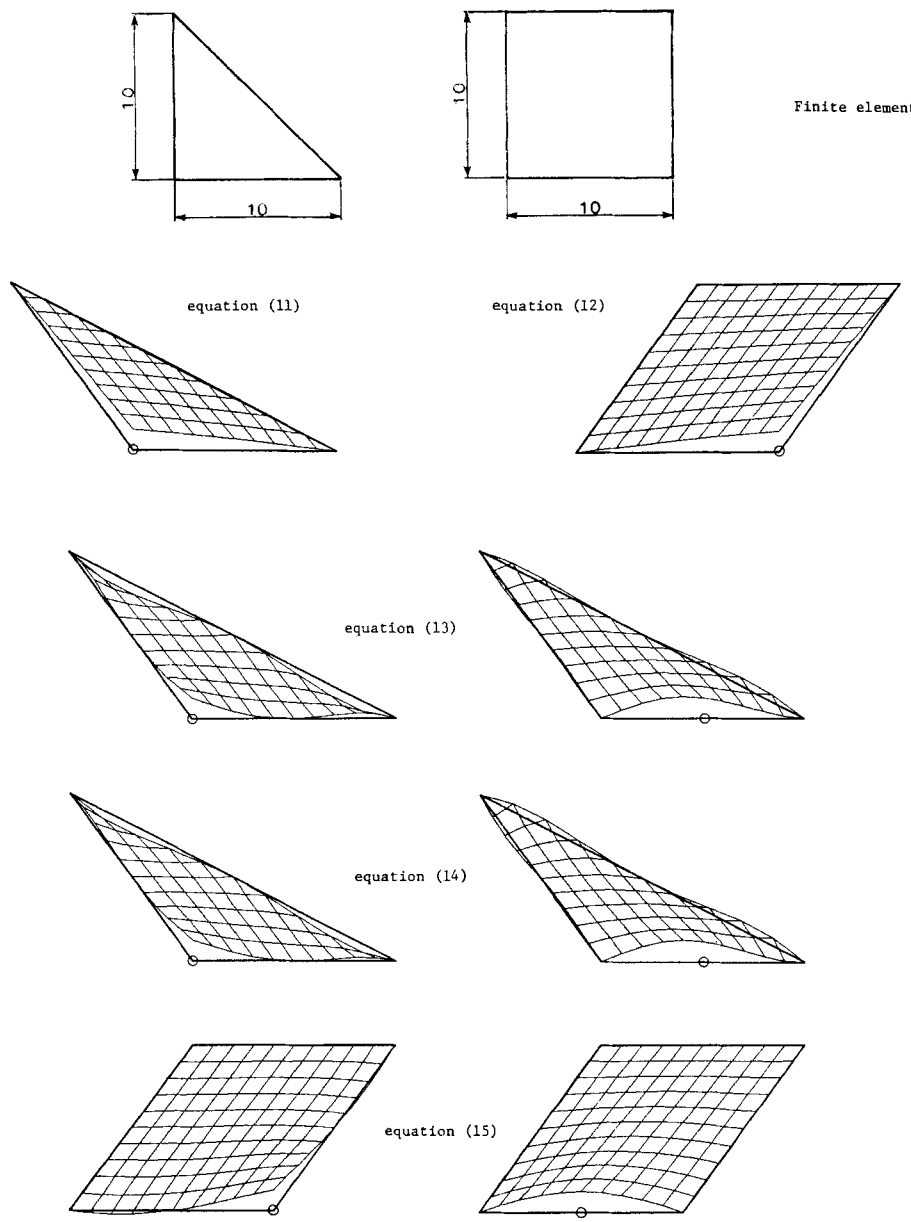

Figure 2. Interpolation equation

the interpolation equation. However, the inverse of **G** in equation (7) sometimes cannot be computed. We have shown numerically that the inverse of **G** corresponding to equations (11)–(15) can be derived. The computed results are not completely independent of the co-ordinate system which is attached to the finite element. The co-ordinates used are shown in Figure 1.

Interpolation equation (8), based on equations (11)–(15), is represented in Figure 2. For

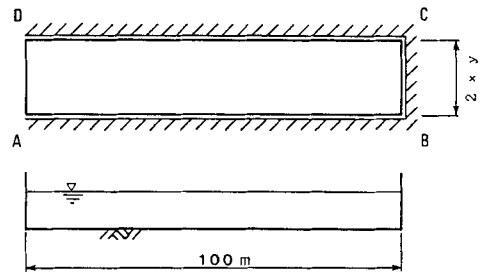

Boundary conditions

$\eta = 1$ on A–D

$\eta_{,n} = 0$ on A–B–C–D

Figure 3. Water channel and boundary condition

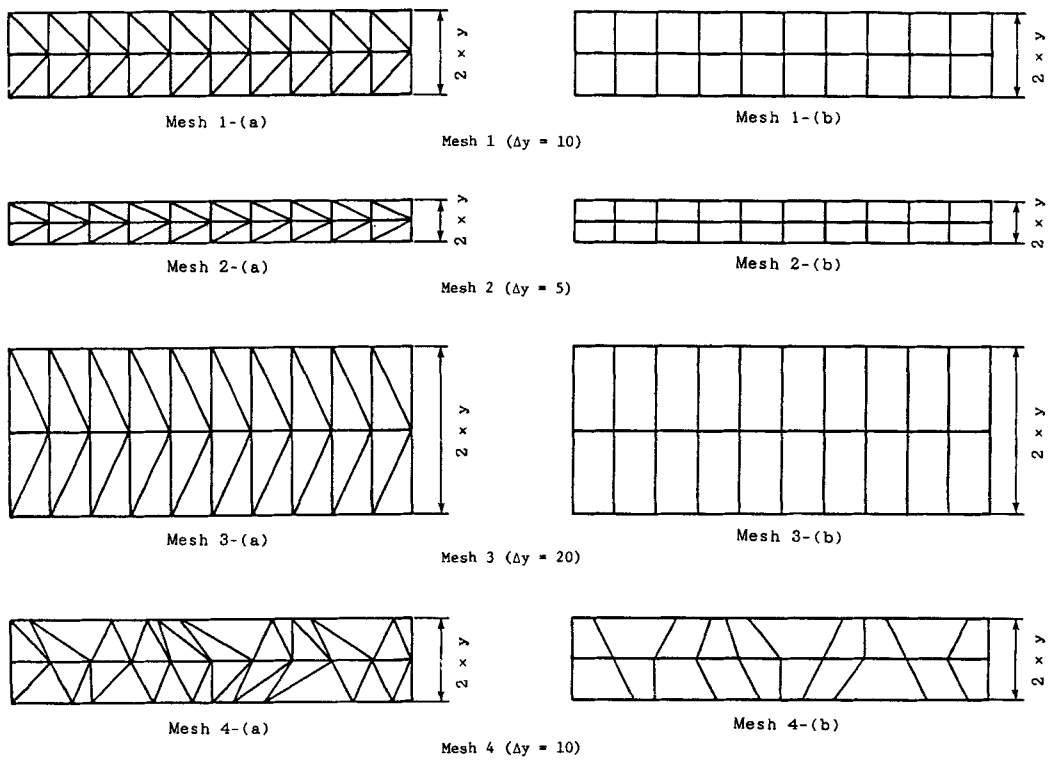

Figure 4. Finite element mesh

illustration, equilateral rectangular–triangular and square elements are used. For wave number k, the following values are used: $k=4\pi/100$ for the three-node triangular and four-node quadrilateral elements; $k=8\pi/100$ for the six-node triangular and eight-node quadrilateral elements. The interpolation equations are illustrated according to a nodal value of $\tilde{\eta}$ at a nodal point 1. Figure 2 shows that the interpolation equation is not always zero along the sides of the element, which means that the interpolation equations on both sides of adjoint elements are not coincident with each other; in other words, all elements are non-conforming elements. This fact means that six-node and eight-node elements are not necessarily an improvement over three-node and four-node elements.

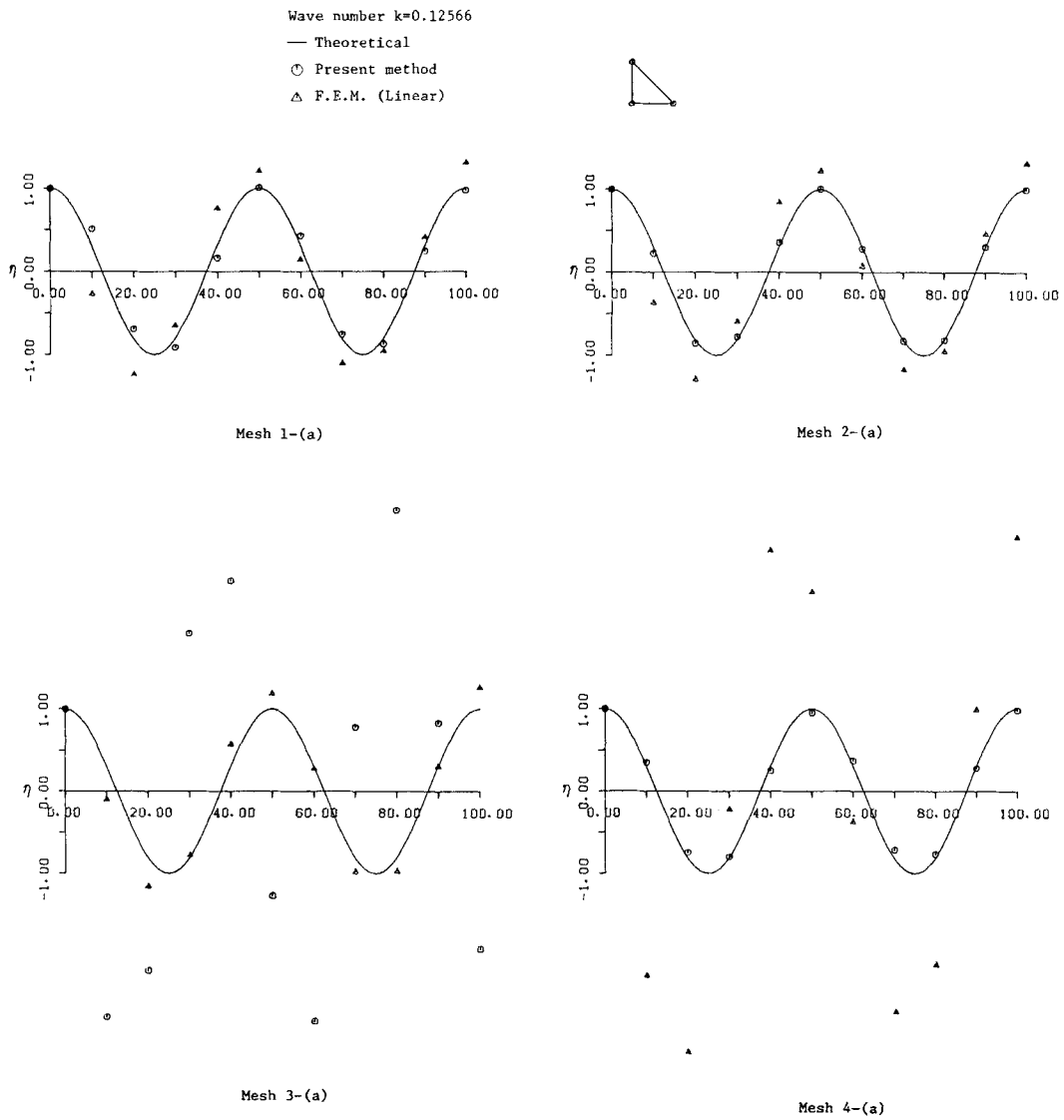

Figure 5. Computed results based on three-node triangular element with equation (11)

WATER OSCILLATION OF CONSTANT-DEPTH CHANNEL

For a comparative study we have analysed the oscillation of water in an open channel assuming a constant water depth. In this case the Helmholz equation is used as the basic equation. Figure 3 shows the configuration of the channel and the boundary conditions imposed. The water elevation is specified as 1. on the boundary A–D and the normal derivative of the water elevation, $\eta_{,n}=0$, is assumed on the boundary A–B–C–D. Numerical studies based on four types of mesh pattern (Figure 4) have been carried out. Mesh 1 is the standard mesh pattern which consists of equilateral rectangular–triangular or square elements, referred to as mesh 1-(a) and mesh 1-(b) respectively. In meshes 2 and 3 the widths of the channels are chosen to be half and twice that of the standard mesh pattern respectively. Mesh 4 is an irregular pattern of the finite element idealizaton.

The computed elevations with $k=4\pi/100$ are plotted in Figures 5 and 6. The computations have been carried out using equation (11), based on the three-node triangular element, and equation (12), based on the four-node quadrilateral element. Numerical results obtained for

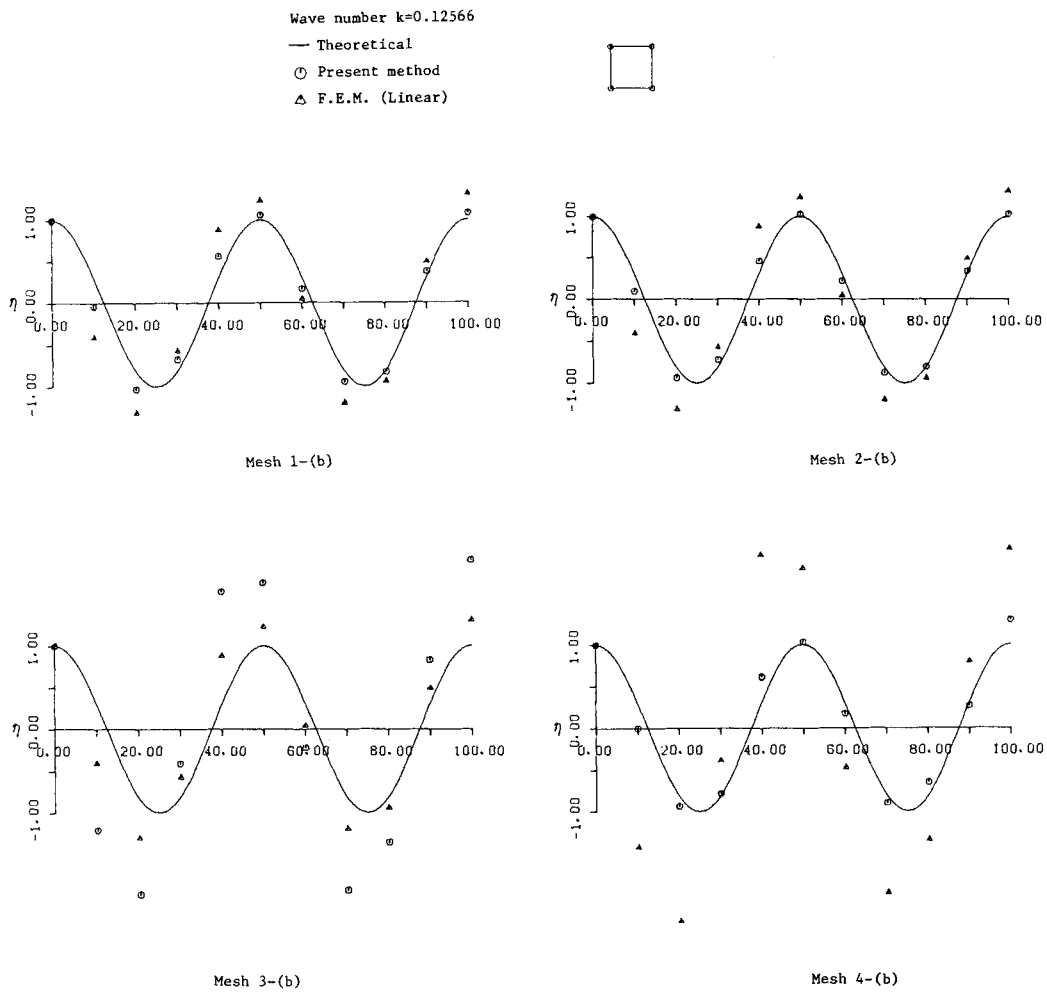

Figure 6. Computed results based on four-node quadrilateral element with equation (12)

meshes 1–4 are shown by circles, while those obtained for conventional linear triangular and bilinear quadrilateral elements are shown by triangles. The solid curve shows the analytical solution. Close agreement is seen between the numerical results obtained by the present method and the analytical solution. However, in the case of the results for mesh 3, for both triangular and quadrilateral elements, there is a slight discrepancy between the numerical and analytical solutions, seemingly because the constant wave field cannot be expressed by the interpolation

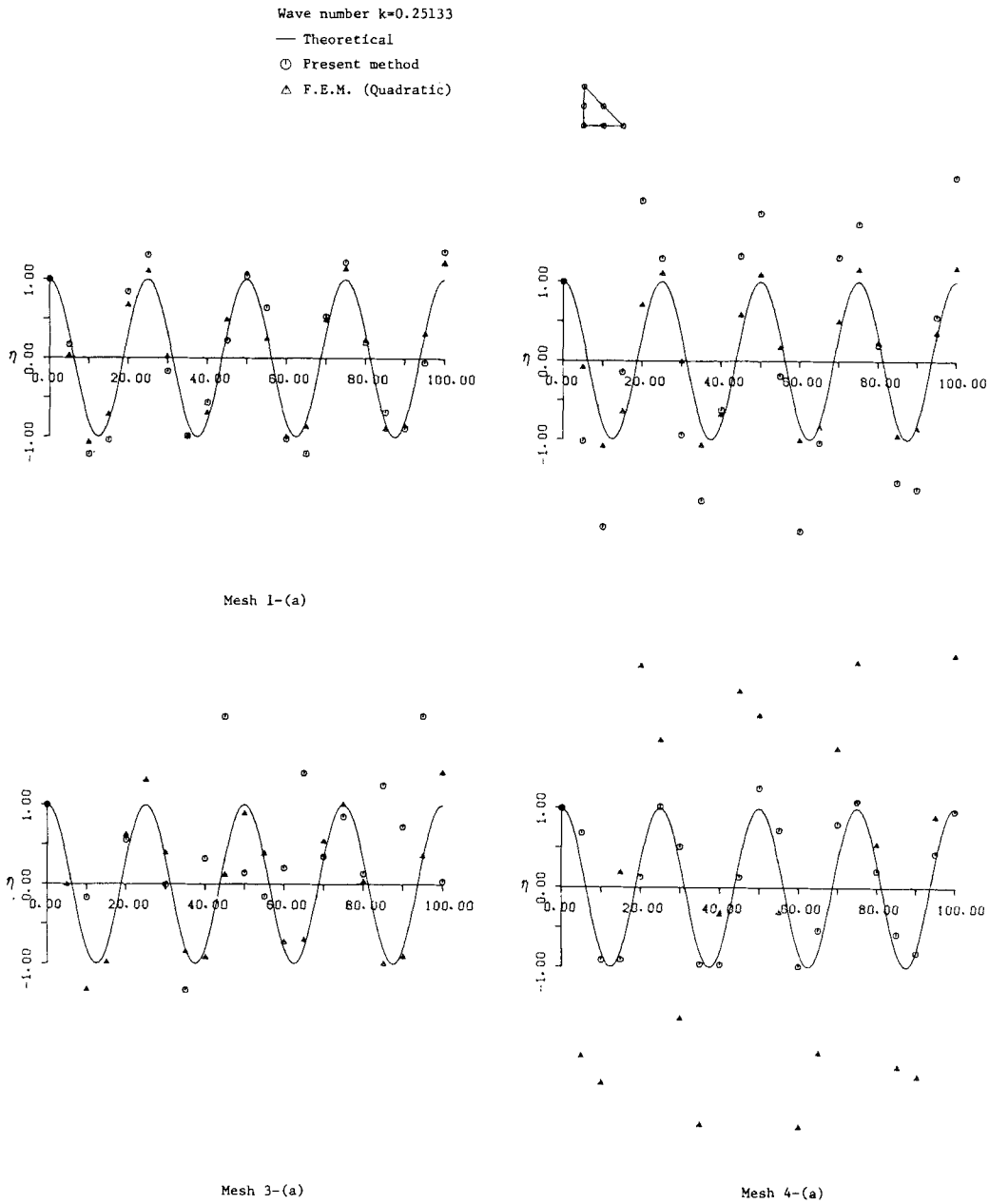

Figure 7. Computed results based on six-node triangular element with equation (13)

equations employed in this paper. In our computed results the numerical solution obtained by the present method is closer to the analytical solution than that obtained by the conventional method.

The computed elevations with $k = 8\pi/100$ are illustrated in Figures 7–9. The computations have been carried out using equations (13) and (14), based on the six-node triangular element, and equation (15), based on the eight-node quadrilateral element. Unfortunately, the numerical results

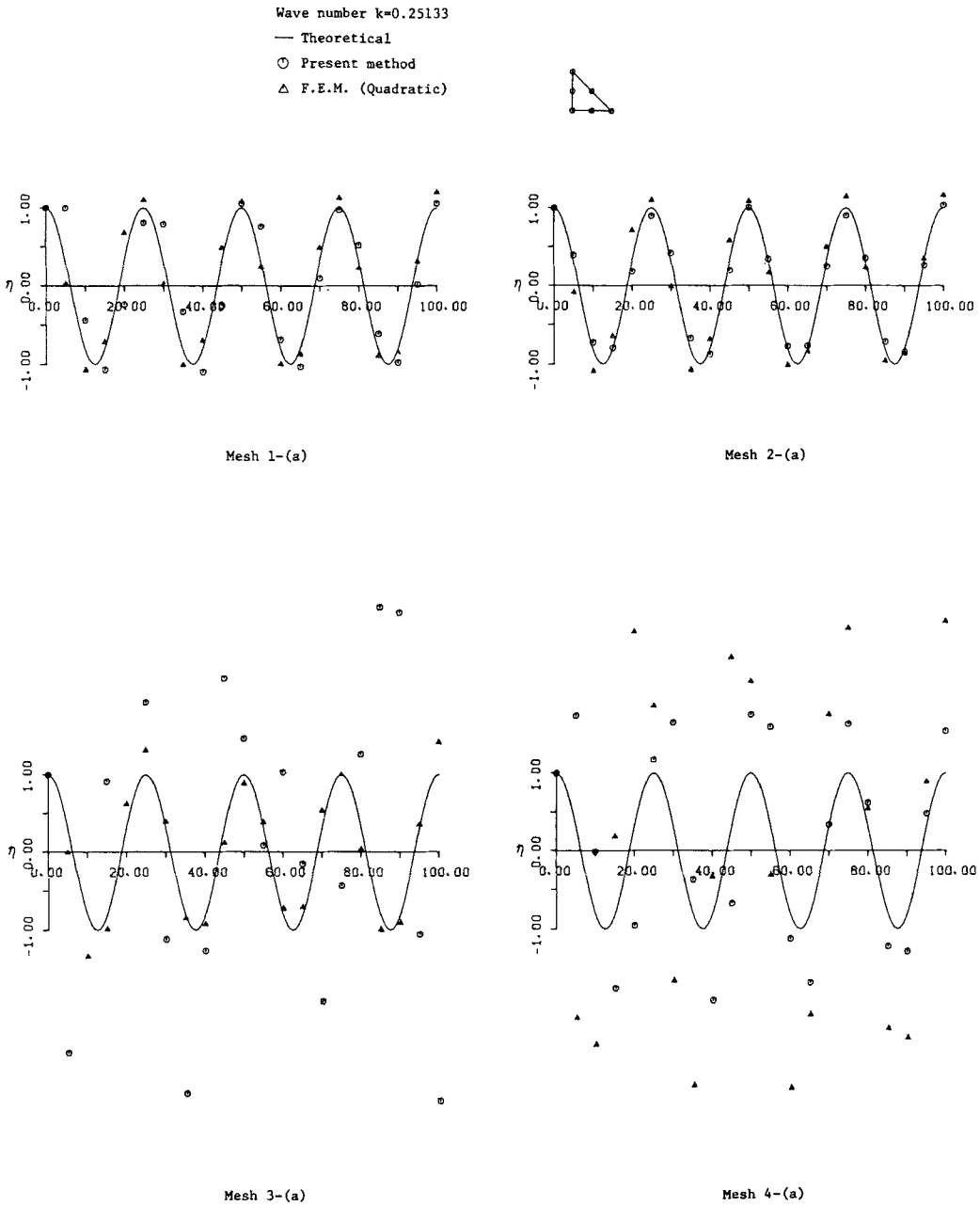

Figure 8. Computed results based on six-node triangular element with equation (14)

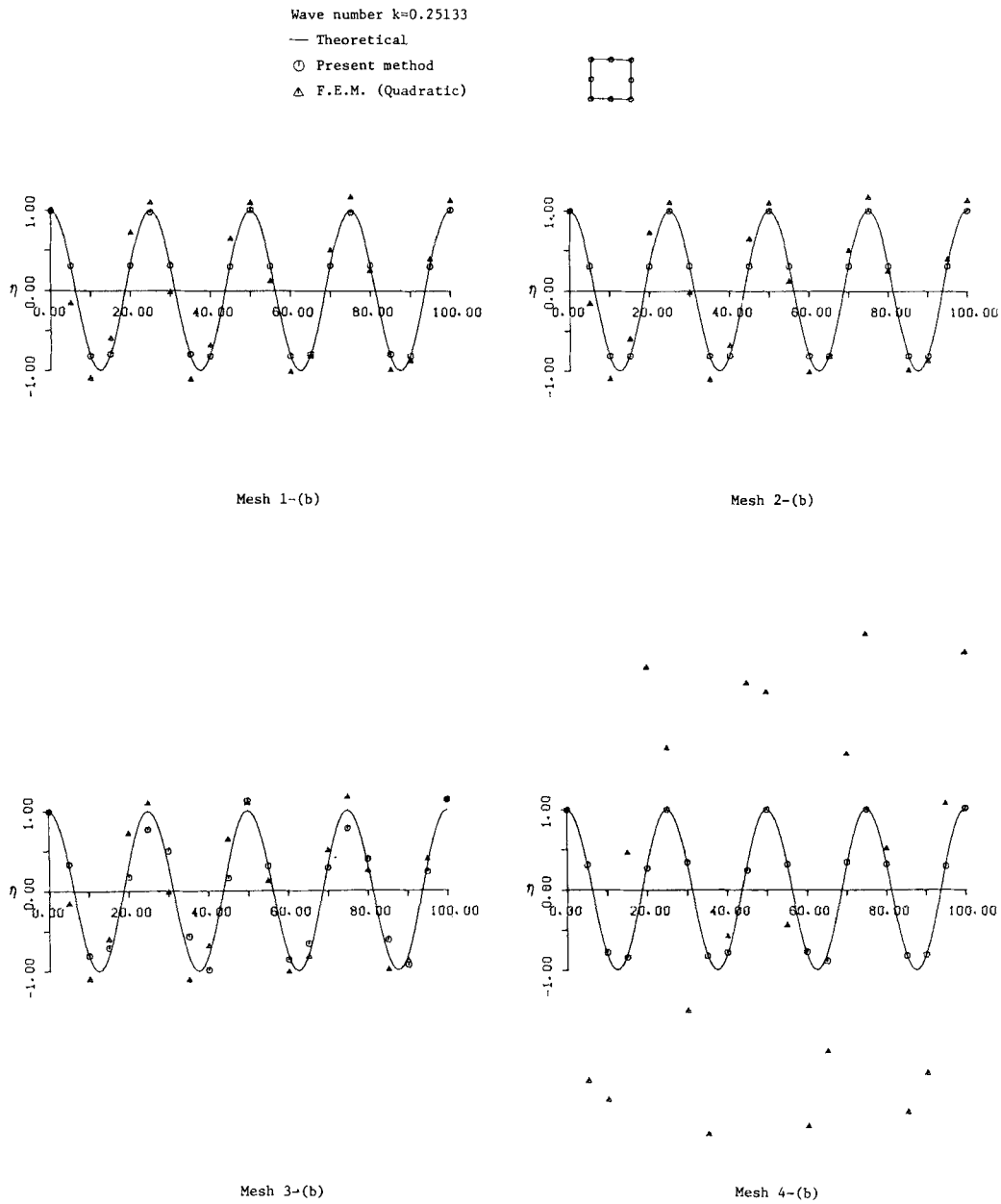

Figure 9. Computed results based on eight-node quadrilateral element with equation (15)

shown in Figures 7 and 8 are not in good agreement with the analytical solution; we therefore abandoned the use of the six-node triangular elements. As shown in Figure 9, the water elevation computed by the eight-node quadrilateral element is in good agreement with the analytical solution.

WATER OSCILLATION OF INCLINED-BOTTOM CHANNEL

In the light of the results of the previous section, we have studied three types of interpolation equation, (11), (12) and (15), for the oscillation of water in an open channel with an inclined water depth as shown in Figure 10. The boundary conditions are also shown in the figure. Three types of finite element mesh pattern have been used, referred to as meshes 1, 2 and 3. The computation has been carried out with a wave period $T = 25{\cdot}73$ s. The numerical wave elevations are illustrated in Figures 11–14. The circles are the results obtained by the present method and the triangles those obtained by linear triangular or bilinear quadrilateral elements. The solid curve shows the analytical solution.[8] The numerical solutions derived by equation (11), based on the three-node triangular element, and by equation (12), based on the four-node quadrilateral element, are in good agreement with the analytical solutions as shown in Figures 11 and 12. Contrary to this, the results by the eight-node quadrilateral element using mesh 3 show a marked discrepancy from the analytical solution as shown in Figure 13. For comparison, the computation has also been performed using mesh 2, i.e., the finer finite element idealization, the results of which are shown in Figure 14. The results are not improved and there are discrepancies between the numerical and analytical solutions. Moreover, the computation must be carried out with double precision, otherwise computation errors lead to a non-realistic solution. This fact is quite inconvenient for practical computation.

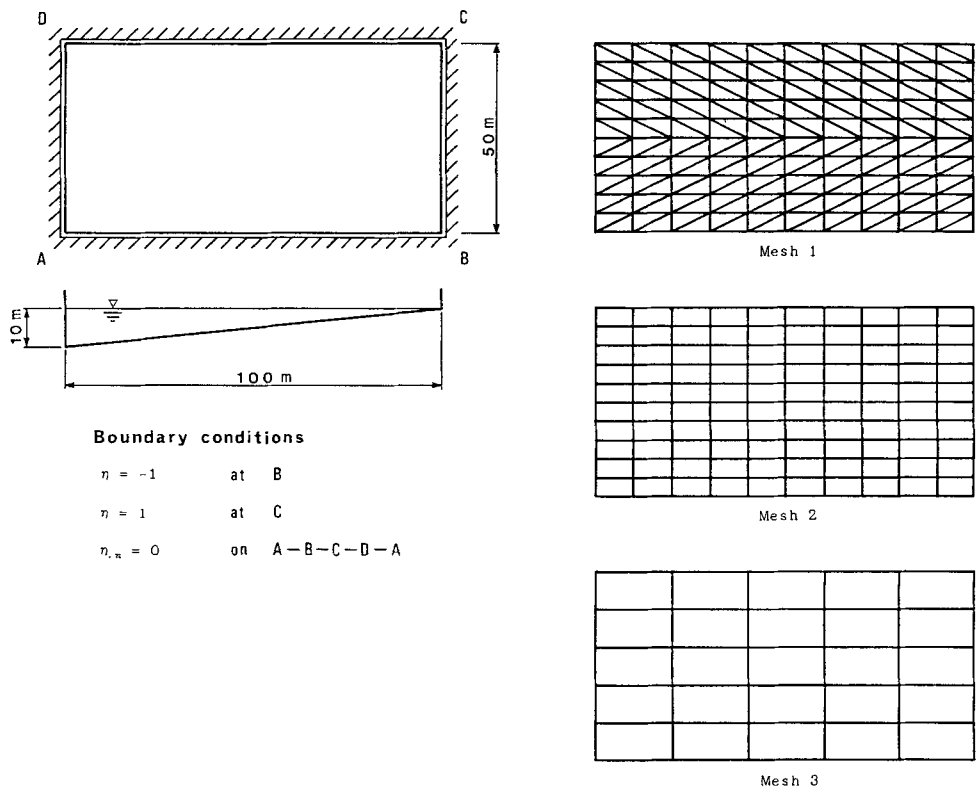

Figure 10. Water channel and finite element idealization

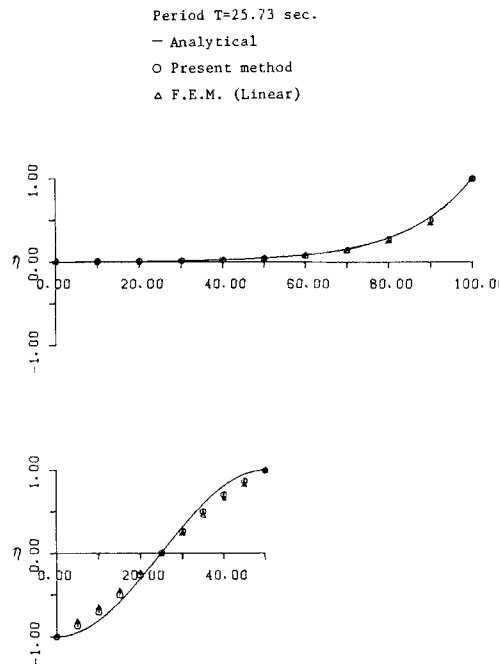

Figure 11. Mesh 1 with three-node triangular element

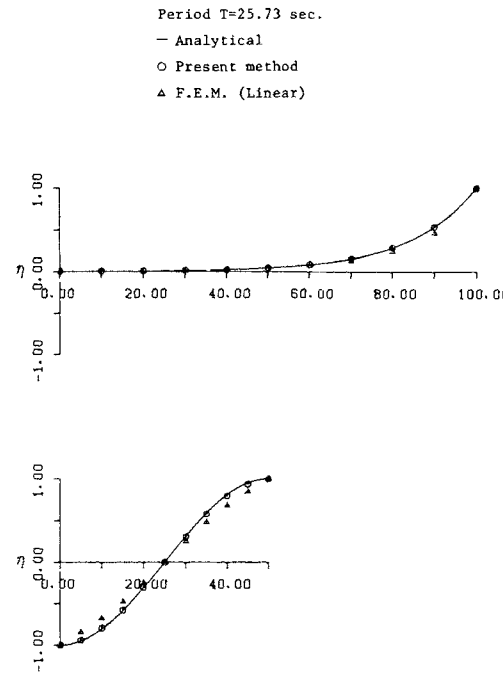

Figure 12. Mesh 2 with four-node quadrilateral element

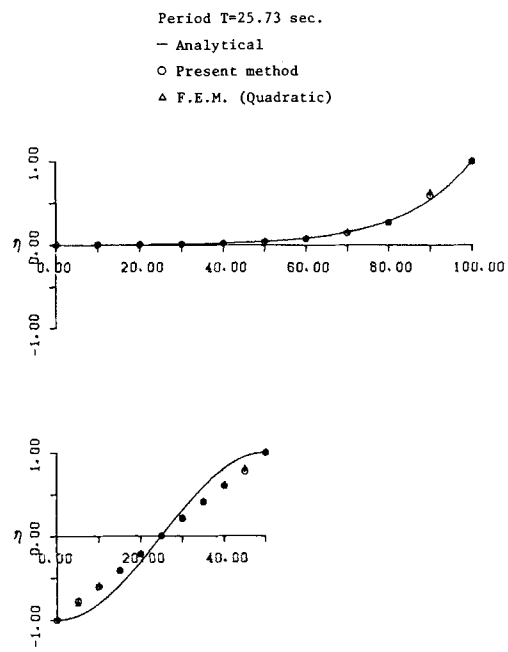

Figure 13. Mesh 3 with eight-node quadrilateral element

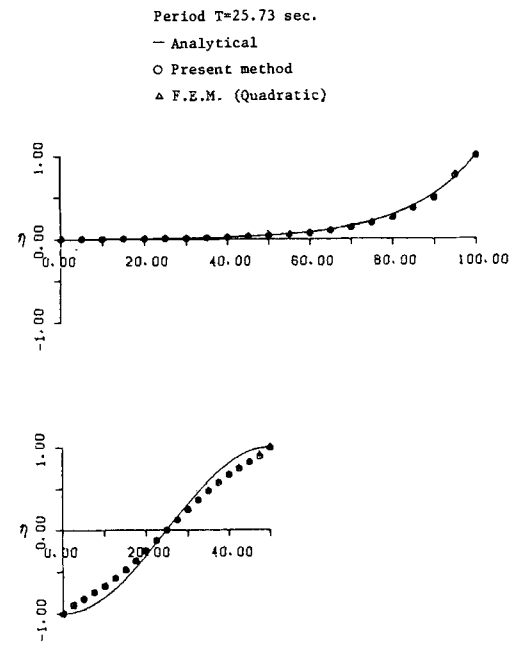

Figure 14. Mesh 2 with eight-node quadrilateral element

OSCILLATION OF OHFUNATO BAY

As a practical application, an oscillation analysis of Ohfunato Bay has been conducted. Various observations were made recently and there are plenty of observed data on the oscillation period in this bay. In the light of the results of the previous two sections, the interpolation functions of the three-node triangular and four-node quadrilateral elements have been chosen for the computations. Figures 15 and 16 show the finite element idealizations used. The total numbers of nodes and elements are 349 and 536 in the case of the three-node triangular element and 349 and 268 in the case of the four-node quadrilateral element respectively. At locations C and D breakwaters are constructed. The contour lines of water depth are represented in Figure 17. The boundary conditions that $\eta = 1.$ on the boundary A–B and $\eta_{,n} = 0$ on the boundary A–C–E–D–B are imposed. The computations have been conducted varying the oscillation period from 1 to 60 min. The computed water elevations at points a and b are plotted in Figure 18 in the case of the three-node element and in Figure 19 in the case of the four-node element. The observed characteristic periods obtained by the tidal gauge along the coastline are 15 and 40 min[9] as shown in Figure 20, which are in good agreement with the computed results. Figures 21 and 22 are illustrations of the oscillation modes at the time when the characteristic periods were 15 and 39 min respectively. The numerical results in Figures 21 and 22 have been obtained by the three-node triangular element. The results by the four-node quadrilateral element are almost coincidental with those in Figures 21 and 22.

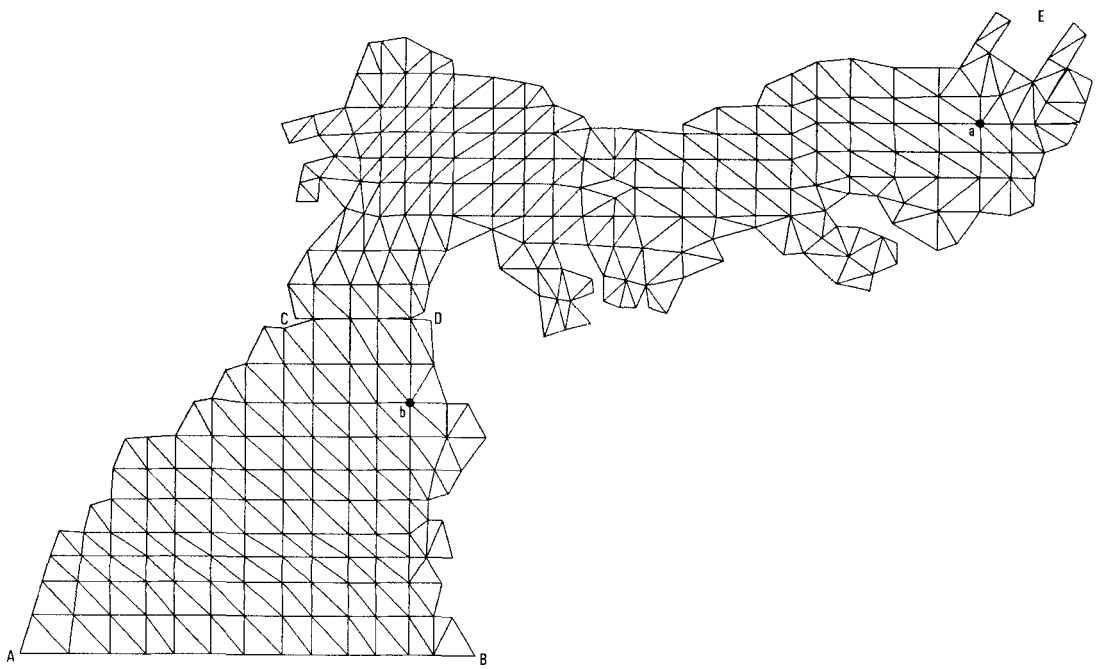

Figure 15. Finite element idealization by three-node triangular element

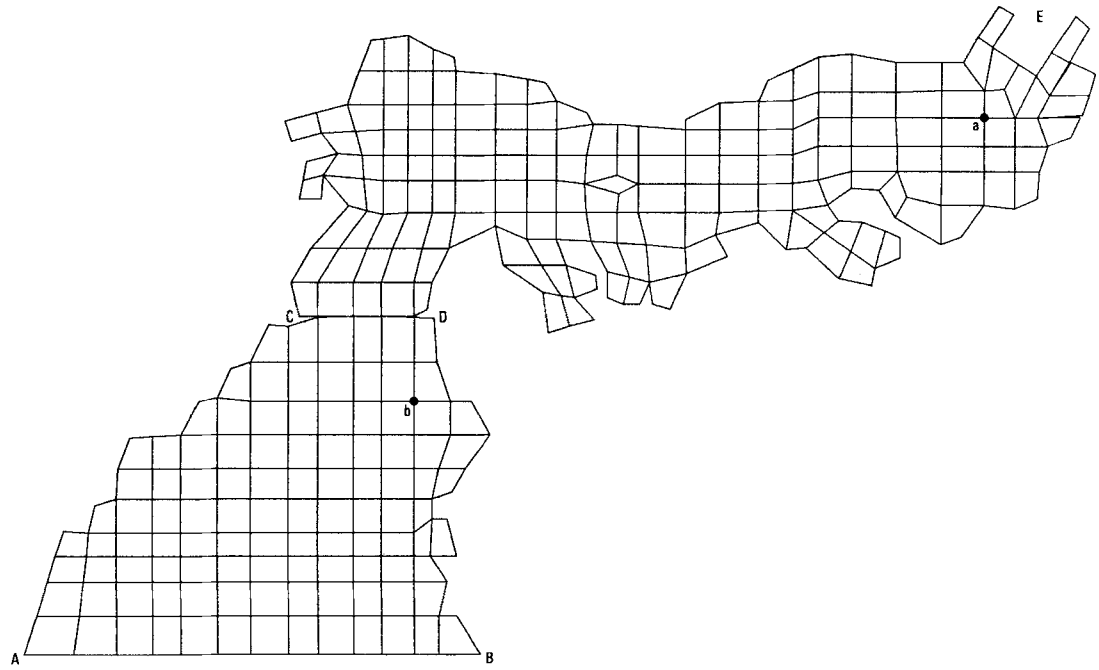

Figure 16. Finite element idealization by four-node quadrilateral element

Figure 17. Contour line of water depth

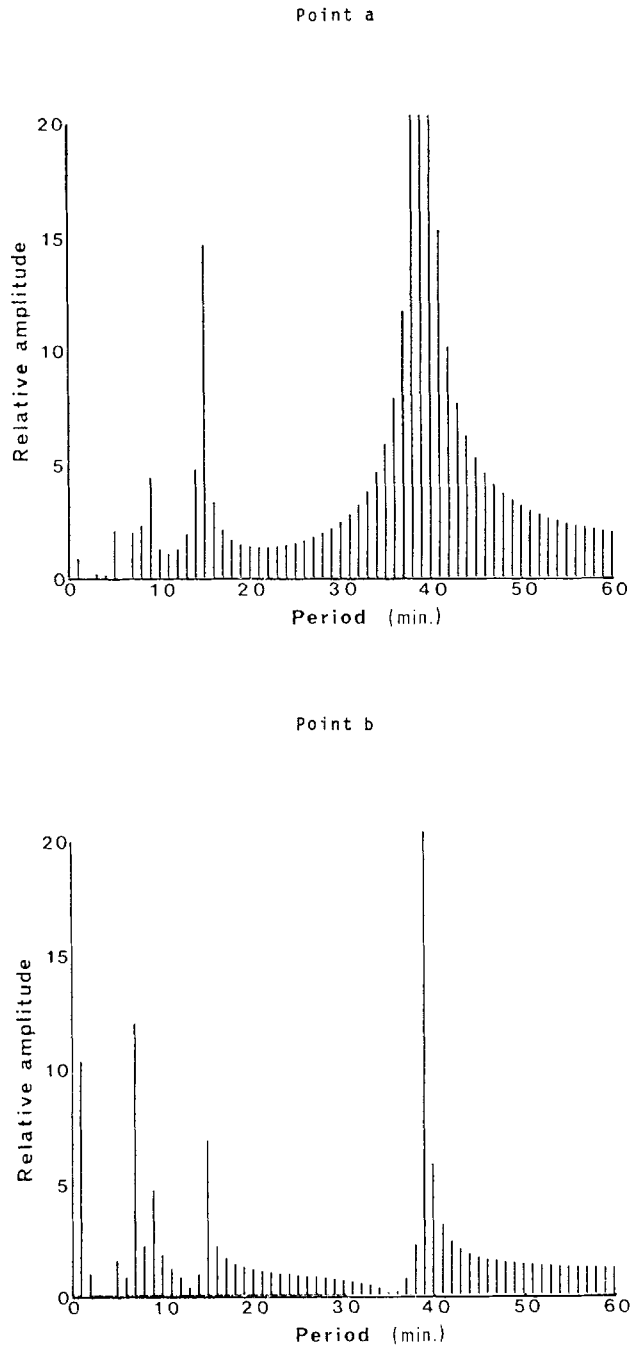

Figure 18. Wave amplitude computed by three-node triangular element

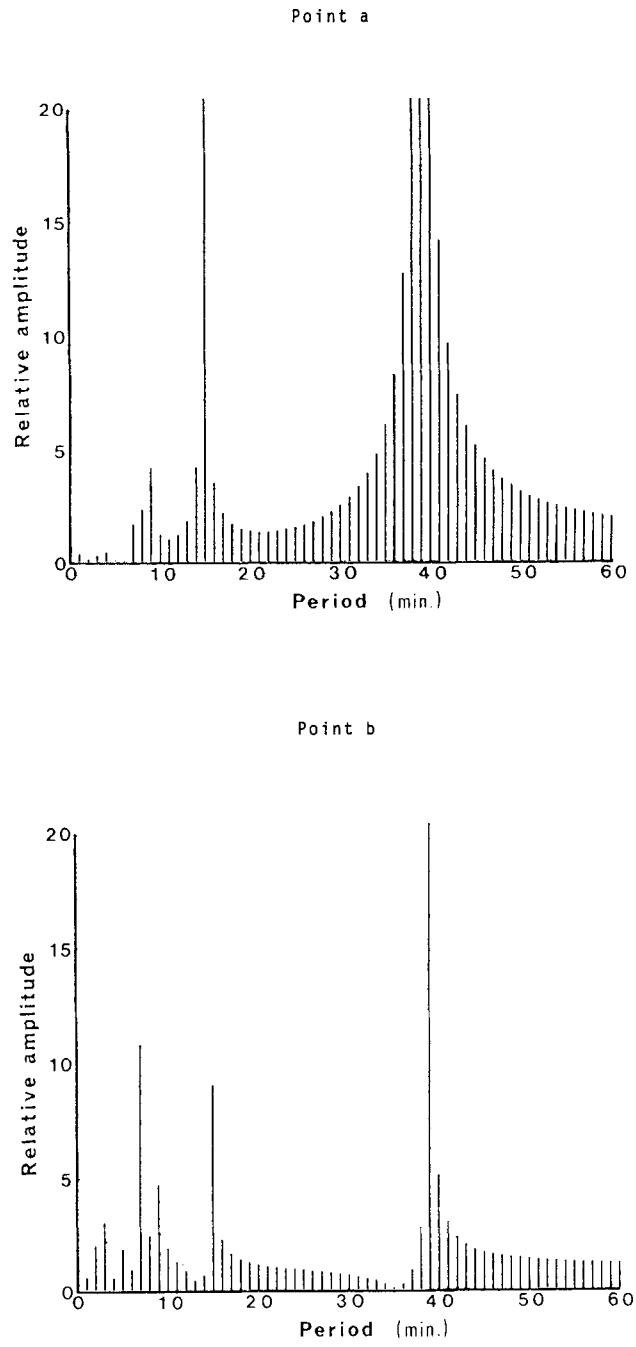

Figure 19. Wave amplitude computed by four-node quadrilateral element

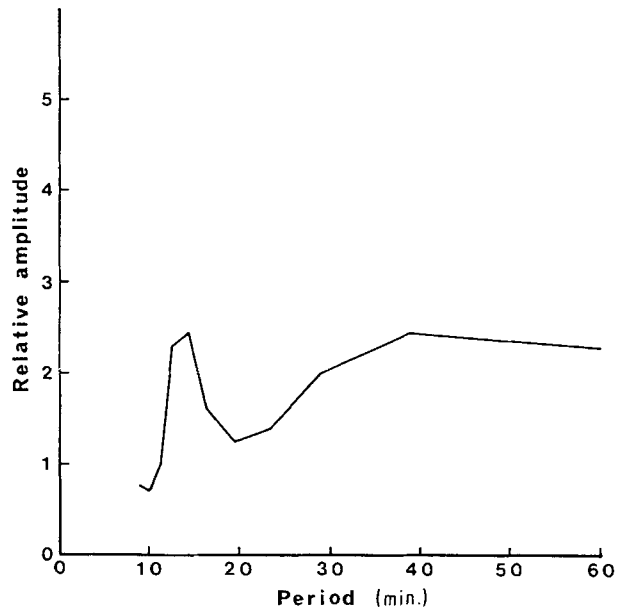

Figure 20. Observed relative amplitude at point a

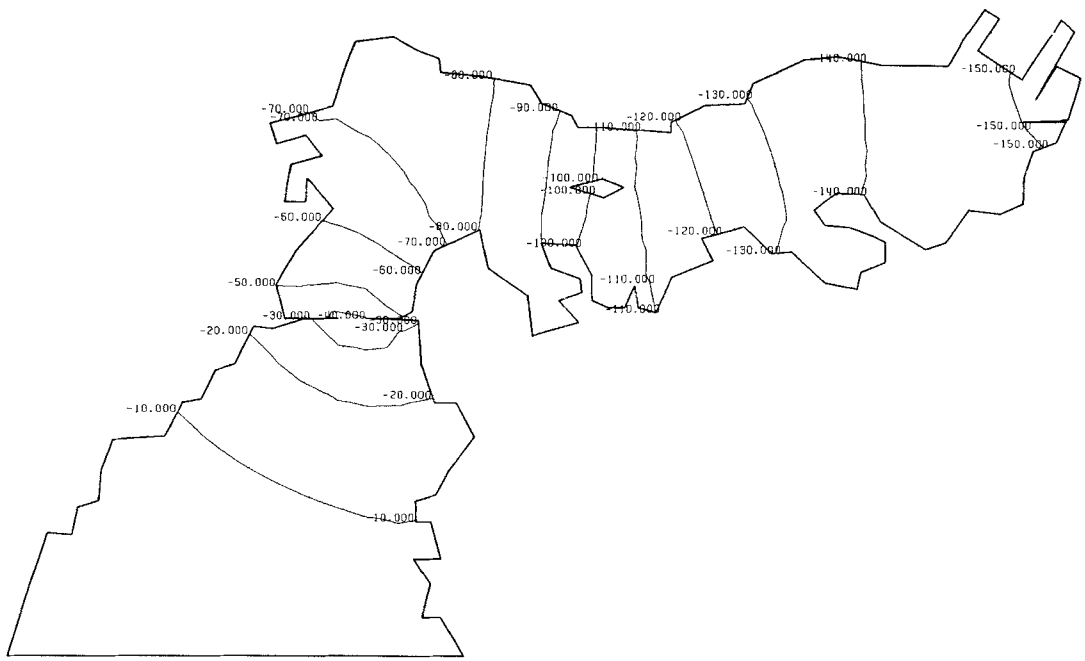

Figure 21. Computed oscillation mode at characteristic period of 15 min

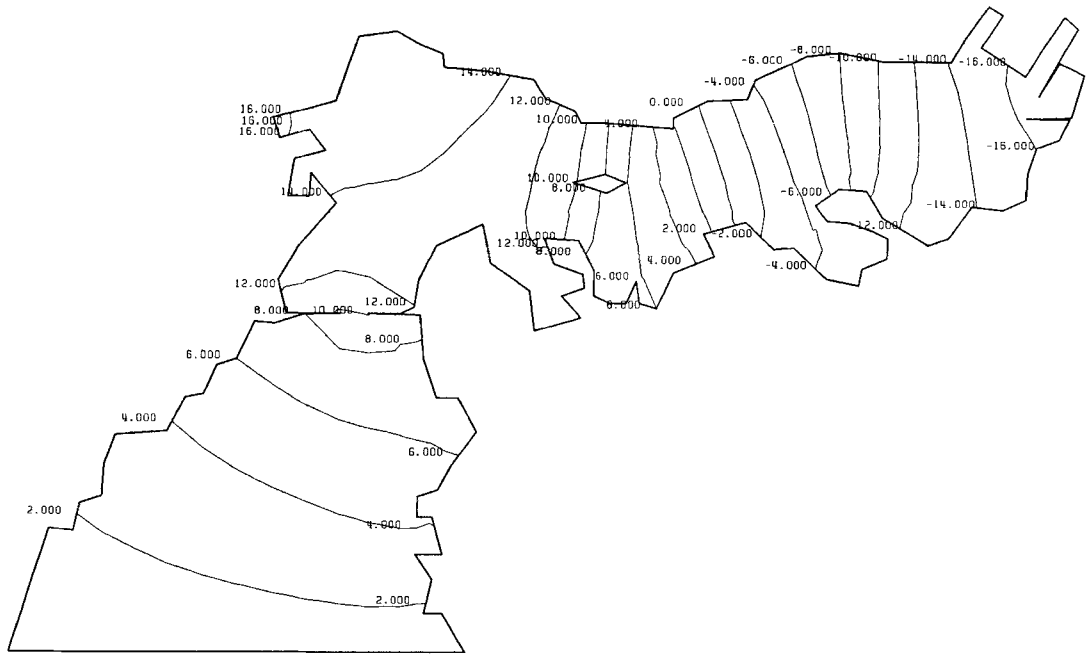

Figure 22. Computed oscillation mode at characteristic period of 39 min

CONCLUSIONS

Five types of interpolation have been tested for the boundary-type finite element method. The conclusions derived are as follows:

(i) All interpolation equations are non-conforming as shown in Figure 2. Thus the multiple-node element is not always better than the simple element.
(ii) According to the numerical results obtained in the constant-depth channel, interpolation equations (13) and (14), based on the six-node triangular element, are not suitable for the computation.
(iii) According to the numerical results obtained in the inclined-bottom channel, interpolation equation (15), based on the eight-node quadrilateral element, needs double-precision computation.
(iv) The fact that interpolation equations (11) and (12), based on the three-node triangular and four-node quadrilateral elements respectively, are suitable for the computation is derived from all three numerical examples.
(v) Numerical results obtained by the three- and four-node elements are in good agreement with the observed results.

From the results in this paper, it is concluded that the boundary-type finite element method based on the three-node and four-node elements provides a useful tool for the practical computation of wave and oscillation analyses.

ACKNOWLEDGEMENTS

The authors are grateful to Dr. Tsukasa Nakayama, Research Associate of Chuo University, for his earnest discussion during the preparation of this paper. The computations in this paper were carried out on the FACOM 170F computer of Chuo University. A part of this research is supported by the Grant in Aid of Scientific Research, Ministry of Education, Government of Japan No. 60550330.

REFERENCES

1. M. Kawahara, K. Kashiyama and A. Tomita, 'Analysis of surface wave in seas by heuristic finite element and boundary element method', in C. Brebbia, T. Futagami and M. Tanaka (eds), *Proc. 5th Int. Conf. on Boundary Elements*, 1983, pp. 1037–1046.
2. M. Kawahara, K. Kashiyama and A. Tomita, 'Heuristic finite element method for analysis of ocean surface waves', in G. Carey and J. T. Oden (eds), *Proc. 5th Int. Conf. on Finite Elements and Flow Problems*, 1984, pp. 7–12.
3. K. Kashiyama, M. Kawahara and H. Sakurai, 'Boundary type finite element method using trigonometric function for water surface wave analysis', *Proc. 4th Int. Conf. on Applied Numerical Modeling*, 1984, pp. 331–335.
4. M. Kawahara and K. Kashiyama, 'Boundary type finite element method for surface wave motion based on trigonometric function interpolation', *Int. j. numer. methods eng.*, **21**, 1833–1852 (1985).
5. K. Kashiyama and M. Kawahara, 'Boundary type finite element method for surface wave problems', *Proc. Japan Soc. Civ. Eng.*, No. 363/II-4, 205–214 (1985).
6. J. C. W. Berkhoff, 'Computation of combined refraction–diffraction', *Proc. 13th Int. Conf. on Coastal Engineering*, Acse 1, 1972, pp. 471–490.
7. R. Smith and T. Spinks, 'Scattering of surface wave by a conical island', *J. Fluid Mech.*, **72** (Part 2), 373–384 (1975).
8. K. Hidaka, 'Tidal oscillations in a rectangular basin of variable water depth', *Geograph. Mag.* **5**, 265–271 (1932).
9. K. Horikawa and H. Nishimura, 'Studies on the effect of breakwater against tsunami waves', *Proc. 16th Japan Coastal Engineering Conf.*, 1969, pp. 365–369 (in Japanese).